

Short Note

(*trans*-Dihydroxo)Sn(IV)-[5,10,15,20-tetrakis(2-pyridyl)porphyrin]

Nirmal Kumar Shee and Hee-Joon Kim * 

Department of Chemistry and Bioscience, Kumoh National Institute of Technology,
Gumi 39177, Republic of Korea

* Correspondence: hjk@kumoh.ac.kr; Tel.: +82-54-4787822

Abstract: Sn(IV)-porphyrin complex with *trans*-dihydroxo axial-ligands and 2-pyridyl peripheral substituents, namely (*trans*-dihydroxo)[5,10,15,20-tetrakis(2-pyridyl)porphyrinato]tin(IV) was synthesized and fully characterized by various techniques such as elemental analysis, ¹H NMR spectroscopy, ESI-MS spectrometry, UV-visible spectroscopy, and fluorescence spectroscopy.

Keywords: porphyrin; tin(IV); hydroxo ligand; 2-pyridyl peripheral substituent

1. Introduction

Sn(IV)-porphyrins are attractive motifs for constructing self-assembled metalloporphyrin nanostructures because they can exhibit unique features by adopting functional ligands in axial positions [1–3]. The role of hydroxo ligands in Sn(IV)-porphyrins has been investigated and exploited from various chemical perspectives. The X-ray structural analysis of (*trans*-dihydroxo)[5,10,15,20-tetrakis(4-pyridyl)porphyrinato]tin(IV) revealed that the hydroxo ligands act as a hydrogen bonding acceptor and the Sn(IV)-porphyrins are supramolecularly assembled into a two-dimensional network through hydrogen bonding [4]. The hydroxo ligand can be readily converted to alcoholic or carboxylic ligands by acidolysis, resulting in various hexacoordinate Sn(IV)-porphyrin complexes that exhibit interesting functions [5–13]. Sn(IV)-porphyrins with additional binding sites enable the creation of sophisticated multiporphyrin arrays [14–16] and nanostructures for application in photocatalysis [17–19]. Here, we report a tin(IV) porphyrin complex with *trans*-dihydroxo axial-ligand and 2-pyridyl peripheral substituents, namely, (*trans*-dihydroxo)[5,10,15,20-tetrakis(2-pyridyl)porphyrinato]tin(IV). Cooperativities between axial ligands and peripheral functional groups in six-coordinated Sn(IV)-porphyrins can lead to various assembled structures for the development of interesting porphyrin materials [20–30].

2. Results and Discussion

The synthetic route used for preparing free-base 5,10,15,20-tetrakis(2-pyridyl)porphyrin (H₂T(2-Py)P) and its Sn(IV) complex (**1**) is shown in Scheme 1. In brief, H₂T(2-Py)P was reacted with tin(II) chloride in pyridine under aerobic conditions followed by hydrolysis to afford **1** in high yield. **1** was fully characterized using various techniques, including elemental analysis, electrospray ionization mass (ESI-MS) spectrometry, ¹H NMR, UV-vis absorption, and fluorescence spectroscopy. The ¹H NMR spectrum of **1** in CDCl₃ is shown in Figure S2. The resonance at −7.34 ppm of much higher field by the strong shielding of porphyrin ring current obviously represents the proton at the axial Sn-OH. On the other hand, the β-pyrrole and α-pyridyl protons of **1** are in the deshielding zone, and their resonances appear at 9.05–9.15 ppm. The remaining protons of the pyridyl group appear at 7.79, 8.17, and 8.35 ppm. ¹³C NMR confirmed the aromatic as well as porphyrinic carbon centers present at **1** as shown in Figure S3. In the FT-IR spectra of **1**, the absorption peaks at 1025 cm^{−1} and 795 cm^{−1} belong to the bending vibration of C-H and the out-of-plane bending vibration of C-H in the aromatic ring, respectively. The peaks at 3050 cm^{−1},



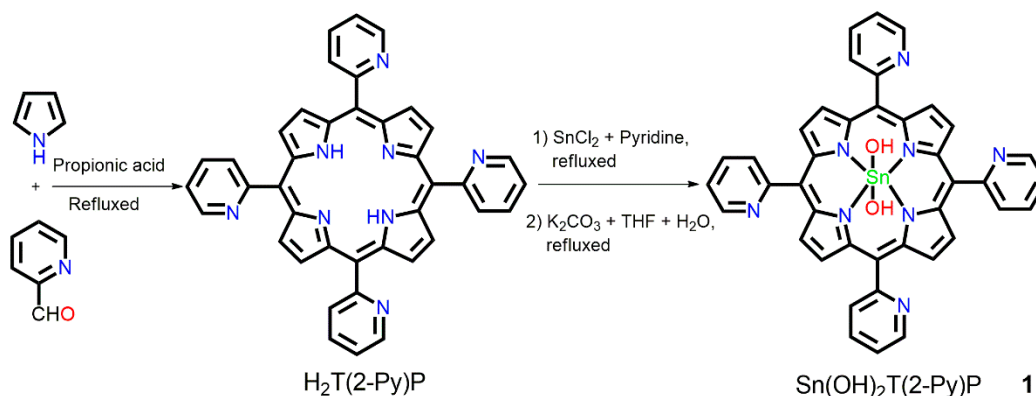
Citation: Shee, N.K.; Kim, H.-J. (*trans*-Dihydroxo)Sn(IV)-[5,10,15,20-tetrakis(2-pyridyl)porphyrin]. *Molbank* **2023**, *2023*, M1669. <https://doi.org/10.3390/M1669>

Received: 6 May 2023
Revised: 2 June 2023
Accepted: 6 June 2023
Published: 14 June 2023



Copyright: © 2023 by the authors. Licensee MDPI, Basel, Switzerland. This article is an open access article distributed under the terms and conditions of the Creative Commons Attribution (CC BY) license (<https://creativecommons.org/licenses/by/4.0/>).

1580 cm^{-1} , and 1430 cm^{-1} are attributed to the stretching vibrations of C-H, C=C, and C-N in the pyrrole ring, respectively. The peaks at 3605 cm^{-1} are assigned to the stretching vibrations of the OH signal of the axial hydroxyl group present in **1**. As shown in Figure S6, a peak at 771.12 is observed in the ESI-MS spectrum of **1**, corresponding to the molecular ion peak $[1 + \text{H}]^+$. The UV-vis absorption of **1** at 427 nm represents the strong Soret band, while the Q-bands appear at 522, 560, and 600 nm (Figure S7). This UV-vis absorption spectral pattern is quite similar to that of 4-pyridyl and 3-pyridyl analogues [5]. The fluorescence of **1** is observed as a two-band emission at 601 and 652 nm, as shown in Figure S8.



Scheme 1. Synthesis of **1**.

3. Materials and Methods

All chemicals were purchased from TCI (Tokyo Chemical Industry Co. LTD, Tokyo, Japan) and used without further purification. Elemental analysis was carried out using an EA 1110 Fisons analyzer (Used Lab Machines Limited, London, England). ^1H NMR spectra were obtained using a Bruker BIOSPIN/AVANCE III 400 spectrometer at 293 K (Bruker BioSpin GmbH, Silberstreifen, Rheinstetten, Germany). Electrospray ionization mass (ESI-MS) spectra were recorded using a Thermo Finnigan linear ion trap quadrupole mass spectrometer (Thermo Fisher Scientific, Waltham, MA, USA). Steady-state UV-Vis and fluorescence spectra were recorded using a Shimadzu UV-3600 and Shimadzu RF-5301PC fluorescence spectrophotometer, respectively (Shimadzu, Tokyo, Japan). FT-IR (Fourier transform infrared spectroscopy) spectra (KBr) were obtained using a Shimadzu FTIR-8400S spectrophotometer (Shimadzu, Tokyo, Japan).

3.1. 5,10,15,20-tetrakis(2-pyridyl)porphyrin $\text{H}_2\text{T}(2\text{-Py})\text{P}$

Freshly distilled pyrrole (1.10 mL, 16 mmol) was added dropwise to a solution of 2-pyridinecarboxaldehyde (1.52 mL, 16 mmol) in propionic acid (300 mL) under reflux. After 4 h, the solvent was evaporated to dryness under reduced pressure. Then, the resulting oily residue was dissolved in 10 mL of *N,N'*-dimethylformamide (DMF) and neutralized by adding 1 mL of triethylamine. Subsequently, the reaction mixture was kept in a refrigerator for 12 h. The solid precipitate was filtered, washed with hot water, and then dried in an oven. The crude compound was purified by column chromatography (SiO_2 , eluent: $\text{CHCl}_3/\text{EtOH} = 95:5$) to afford 5,10,15,20-tetra(2-pyridyl)porphyrin $\text{H}_2\text{T}(2\text{-Py})\text{P}$. The product was recrystallized from CHCl_3/n -hexane to give violet purple crystals. Yield: 0.544 g (22%). Anal. calculated for $\text{C}_{40}\text{H}_{26}\text{N}_8$: C, 77.65; H, 4.24; N, 18.11. Found: C, 77.48; H, 4.57; N, 17.95. ^1H NMR (400 MHz, CDCl_3 , ppm): δ -2.84 (s, 2H, NH), 7.71 (m, 4H, H4-Py), 7.89 (m, 4H, H3-Py), 8.21 (m, 4H, H5-Py), 8.85 (s, 8H, β -pyrrole), 9.14 (s, 4H, H2-Py). UV-vis (CHCl_3): λ_{nm} (log ϵ), 419 (5.73), 516 (4.60), 552 (4.43), 593 (4.15), 650 (4.07). Emission (CHCl_3): λ_{nm} 653, 712.

3.2. Synthesis of (trans-dihydroxo)[5,10,15,20-tetrakis(2-pyridyl)porphyrinato]tin(IV) (**1**)

$\text{H}_2\text{T}(2\text{-Py})\text{P}$ (0.31 g, 0.5 mmol) was dissolved in 40 mL of pyridine, and $\text{SnCl}_2 \cdot 2\text{H}_2\text{O}$ (0.225 g, 1 mmol) was added to the above solution and the mixture was refluxed for 12 h.

After removal of all the volatiles in vacuo, the residue was dissolved in CHCl_3 and filtered through a celite pad to remove the excess SnCl_2 . The filtrate was evaporated, and the solid residue was re-dissolved in a 3:1 mixture of THF and H_2O (80 mL). K_2CO_3 (0.276 g, 2 mmol) was added to the reaction mixture, which was then refluxed for 12 h. After removal of THF under reduced pressure, the mixture was cooled to 10°C until precipitation of a reddish compound. The filtered solid compound was dried in an oven. The crude product was recrystallized from $\text{CHCl}_3/\text{CH}_3\text{CN}$ to give $\text{Sn}(\text{OH})_2\text{T}(2\text{-Py})\text{P}$ (**1**) as a red crystalline compound. Yield: 0.27 g (70%). Anal. calculated for $\text{C}_{40}\text{H}_{26}\text{N}_8\text{O}_2\text{Sn}$: C, 62.44; H, 3.41; N, 14.56; R, 19.59. Found: C, 62.18; H, 3.76; N, 14.43; R, 19.63. ^1H NMR (400 MHz, CDCl_3 , ppm): δ -7.34 (s, 2H, Sn-OH), 7.79 (m, 4H, H4-Py), 8.17 (m, 4H, H3-Py), 8.38 (m, 4H, H5-Py), 9.05–9.15 (m, 12H, β -pyrrole + H2-Py). ^{13}C NMR (400 MHz, CDCl_3 , ppm): δ 122.97, 123.02, 130.79, 132.68, 135.23, 146.60, 149.07, 159.31, 159.63. FT-IR (KBr): 3605, 3050, 1630, 1580, 1565, 1510, 1460, 1430, 1345, 1260, 1210, 1075, 1025, 990, 845, 795, 765, 725, 680, 555 cm^{-1} . UV-vis (CHCl_3): λ_{nm} (log ϵ), 427 (5.70), 522 (3.65), 560 (4.30), 600 (4.10). Emission (CHCl_3): λ_{nm} 601, 652.

4. Conclusions

A tin(IV) porphyrin complex with *trans*-dihydroxo axial-ligands and 2-pyridyl peripheral substituents was synthesized and characterized by elemental analysis, ^1H and ^{13}C NMR spectroscopy, FT-IR spectroscopy, ESI-MS spectrometry, UV-visible spectroscopy, and fluorescence spectroscopy. This work can contribute to the design and synthesis of novel macrocyclic compounds for recognizing important biomolecules.

Supplementary Materials: Figures S1 and S2: ^1H NMR spectra of free-base porphyrin and **1**, Figure S3: ^{13}C NMR spectrum of **1**, Figure S4: FTIR spectrum of **1**, Figures S5 and S6: ESI-MS spectra of free-base porphyrin and **1**, Figure S7: UV-vis absorption spectra of free-base porphyrin and **1**, Figure S8: Fluorescence spectra of free-base porphyrin and **1**.

Author Contributions: Methodology, software, validation, formal analysis, investigation, data curation, visualization, writing—original draft preparation, N.K.S.; conceptualization, resources, writing—review and editing, project administration, funding acquisition, H.-J.K. All authors have read and agreed to the published version of the manuscript.

Funding: This work was supported by the Kumoh National Institute of Technology (2022).

Institutional Review Board Statement: Not applicable.

Informed Consent Statement: Not applicable.

Acknowledgments: We acknowledge Mihee Lee for the initial synthetic work.

Conflicts of Interest: The authors declare no conflict of interest.

Sample Availability: Not available.

References

1. Arnold, D.P.; Blok, J. The coordination chemistry of tin porphyrin complexes. *Coord. Chem. Rev.* **2004**, *248*, 299–319. [[CrossRef](#)]
2. Shee, N.K.; Lee, C.-J.; Kim, H.-J. Hexacoordinated Sn(IV) porphyrin-based square-grid frameworks exhibiting selective uptake of CO_2 over N_2 . *Bull. Korean Chem. Soc.* **2022**, *43*, 103–109. [[CrossRef](#)]
3. Shee, N.K.; Jo, H.J.; Kim, H.-J. Coordination framework materials fabricated by the self-assembly of Sn(IV) porphyrins with Ag(I) ions for the photocatalytic degradation of organic dyes in wastewater. *Inorg. Chem. Front.* **2022**, *9*, 1270–1280. [[CrossRef](#)]
4. Jo, H.-J.; Jung, S.-H.; Kim, H.-J. Synthesis and Hydrogen-Bonded Supramolecular Assembly of *trans*-Dihydroxotin(IV) Tetrapyrrolylporphyrin Complexes. *Bull. Korean Chem. Soc.* **2004**, *25*, 1869–1873.
5. Fallon, G.D.; Langford, S.J.; Lee, M.A.-P.; Lygris, E. Self-assembling Mixed Porphyrin Trimers—The Use of Diaxial Sn(IV) Porphyrin Phenolates as an Organising Precept. *Inorg. Chem. Commun.* **2002**, *5*, 715–718. [[CrossRef](#)]
6. Hawley, J.C.; Bampos, N.; Sanders, J.K.M. Synthesis and Characterization of Carboxylate Complexes of Sn^{IV} Porphyrin Monomers and Oligomers. *Chem. Eur. J.* **2003**, *9*, 5211–5222. [[CrossRef](#)]
7. Ou, Z.; E, W.; Zhu, W.; Thordarson, P.; Sintic, P.J.; Crossley, M.J.; Kadish, K.M. Effect of Axial Ligands and Macrocyclic Structure on Redox Potentials and Electron-Transfer Mechanisms of Sn(IV) Porphyrins. *Inorg. Chem.* **2007**, *46*, 10840–10849. [[CrossRef](#)]

8. Shetti, V.S.; Ravikanth, M. Sn(IV) Porphyrin based axial-bonding type porphyrin triads containing heteroporphyrins as axial ligands. *Inorg. Chem.* **2010**, *49*, 2692–2700. [[CrossRef](#)]
9. Shetti, V.S.; Ravikanth, M. A simple alternative method for preparing Sn(IV) porphyrins. *J. Porphyrins Phthalocyanines* **2010**, *14*, 361–370. [[CrossRef](#)]
10. Shetti, V.S.; Ravikanth, M. Supramolecular tetrads containing Sn(IV) porphyrin, Ru(II) porphyrin, and expanded porphyrins assembled using complementary metal–ligand interactions. *Inorg. Chem.* **2011**, *50*, 1713–1722. [[CrossRef](#)]
11. Sharma, R.; Ghosh, A.; Wolfram, B.; Bröring, M.; Ravikanth, M. Synthesis and Characterization of Hexa-Coordinated Sn(IV) Complexes of Meso-Aryl Dipyrins. *Dalton Trans.* **2013**, *42*, 5627–5630. [[CrossRef](#)]
12. Pareek, Y.; Lakshmi, V.; Ravikanth, M. Axially bonded pentads constructed on the Sn(IV) porphyrin scaffold. *Dalton Trans.* **2014**, *43*, 6870–6879. [[CrossRef](#)]
13. Natali, M.; Amati, A.; Demitri, N.; Iengo, E. Formation of a Long-Lived Radical Pair State in a Sn(IV) Porphyrin-di-(L-tyrosinato) Conjugate Driven by Proton-Coupled Electron-Transfer. *Chem. Commun.* **2018**, *54*, 6148–6152. [[CrossRef](#)]
14. Shetti, V.S.; Pareek, Y.; Ravikanth, M. Sn(IV) Porphyrin Scaffold for Multiporphyrin Arrays. *Coord. Chem. Rev.* **2012**, *256*, 2816–2842. [[CrossRef](#)]
15. Dvivedi, A.; Pareek, Y.; Ravikanth, M. Sn^{IV} Porphyrin Scaffolds for Axially Bonded Multiporphyrin Arrays: Synthesis and Structure Elucidation by NMR Studies. *Chem. Eur. J.* **2014**, *20*, 4481–4490. [[CrossRef](#)]
16. Amati, A.; Cavigli, P.; Demitri, N.; Natali, M.; Indelli, M.T.; Iengo, E. Sn(IV) Multiporphyrin Arrays as Tunable Photoactive Systems. *Inorg. Chem.* **2019**, *58*, 4399–4411. [[CrossRef](#)]
17. Shee, N.K.; Kim, H.-J. Morphology-controlled self-assembled nanostructures of complementary metalloporphyrin triads obtained through tuning their intermolecular coordination and their photocatalytic degradation of Orange II dye. *Inorg. Chem. Front.* **2022**, *9*, 5538–5548. [[CrossRef](#)]
18. Shee, N.K.; Kim, H.-J. Sn(IV)-Porphyrin-Based Nanostructures Featuring Pd(II)-Mediated Supramolecular Arrays and Their Photocatalytic Degradation of Acid Orange 7 Dye. *Int. J. Mol. Sci.* **2022**, *23*, 13702. [[CrossRef](#)]
19. Shee, N.K.; Kim, H.-J. Supramolecular squares of Sn(IV)porphyrins with Re(I)-corners for the fabrication of self-assembled nanostructures performing photocatalytic degradation of Eriochrome Black T dye. *Inorg. Chem. Front.* **2023**, *10*, 174–183. [[CrossRef](#)]
20. Bhosale, S.V.; Chong, C.; Forsyth, C.; Langford, S.J.; Woodward, C.P. Investigations of rotamers in diaxial Sn(IV)porphyrin phenolates—Towards a molecular timepiece. *Tetrahedron* **2008**, *64*, 8394–8401. [[CrossRef](#)]
21. Lazarides, T.; Kuhri, S.; Charalambidis, G.; Panda, M.K.; Guldi, D.M.; Coutsolelos, A.G. Electron vs Energy Transfer in Arrays Featuring Two Bodipy Chromophores Axially Bound to a Sn(IV) Porphyrin *via* a Phenolate or Benzoate Bridge. *Inorg. Chem.* **2012**, *51*, 4193–4204. [[CrossRef](#)] [[PubMed](#)]
22. Manke, A.M.; Geisel, K.; Fetzer, A.; Kurz, P. A Water-Soluble Tin(IV) Porphyrin as a Bioinspired Photosensitizer for Light-Driven Proton-Reduction. *Phys. Chem. Chem. Phys.* **2014**, *16*, 12029–12042. [[CrossRef](#)] [[PubMed](#)]
23. Kurimoto, K.; Yamazaki, T.; Suzuri, Y.; Nabetani, Y.; Onuki, S.; Takagi, S.; Shimada, T.; Tachibana, H.; Inoue, H. Hydrogen evolution coupled with photochemical oxygenation of cyclohexene with water sensitized by Tin (IV) porphyrins by visible light. *Photochem. Photobiol. Sci.* **2014**, *13*, 154–156. [[CrossRef](#)] [[PubMed](#)]
24. Alka, A.; Pareek, Y.; Shetti, V.S.; Rajeswara Rao, M.; Theophall, G.G.; Lee, W.-Z.; Lakshmi, K.V.; Ravikanth, M.V. Construction of Novel Cyclic Tetrads by Axial Coordination of Thiaporphyrins to Tin(IV) Porphyrin. *Inorg. Chem.* **2017**, *56*, 13913–13929. [[CrossRef](#)] [[PubMed](#)]
25. Ravikumar, M.; Raghav, D.; Rathinasamy, K.; Kathiravan, A.; Mothi, E.M. DNA Targeting Long-Chain Alkoxy Appended Tin(IV) Porphyrin Scaffolds: Photophysical and Antimicrobial PDT Investigations. *ACS Appl. Bio Mater.* **2018**, *1*, 1705–1716. [[CrossRef](#)]
26. Ravikumar, M.; Kathiravan, A.; Neels, A.; Mothi, E.M. Tin(IV) Porphyrins Containing β -Substituted Bromines: Synthesis, Conformations, Electrochemistry and Photophysical Evaluation. *Eur. J. Inorg. Chem.* **2018**, *34*, 3868–3877. [[CrossRef](#)]
27. Baral, E.R.; Kim, D.; Lee, S.; Park, M.H.; Kim, J.G. Tin(IV)-Porphyrin Tetracarbonyl Cobaltate: An Efficient Catalyst for the Carbonylation of Epoxides. *Catalysts*. **2019**, *9*, 311. [[CrossRef](#)]
28. Kumar, R.S.; Kim, H.; Mergu, N.; Son, Y.-A. A photocatalytic comparison study between tin complex and carboxylic acid derivatives of porphyrin/TiO₂ composites. *Res. Chem. Intermed.* **2020**, *46*, 313–328. [[CrossRef](#)]
29. Giannoudis, E.; Benazzi, E.; Karlsson, J.; Copley, G.; Panagiotakis, S.; Landrou, G.; Angaridis, P.; Nikolaou, V.; Matthaiaki, C.; Charalambidis, G.; et al. Photosensitizers for H₂ Based on Charged or Neutral Zn and Sn Porphyrins. *Inorg. Chem.* **2020**, *59*, 1611–1621. [[CrossRef](#)]
30. Thomas, A.; Ohsaki, Y.; Nakazato, R.; Kuttassery, F.; Mathew, S.; Remello, S.N.; Tachibana, H.; Inoue, H. Molecular Characteristics of Water-Insoluble Tin-Porphyrins for Designing the One-Photon-Induced Two-Electron Oxidation of Water in Artificial Photosynthesis. *Molecules* **2023**, *28*, 1882. [[CrossRef](#)]

Disclaimer/Publisher’s Note: The statements, opinions and data contained in all publications are solely those of the individual author(s) and contributor(s) and not of MDPI and/or the editor(s). MDPI and/or the editor(s) disclaim responsibility for any injury to people or property resulting from any ideas, methods, instructions or products referred to in the content.